

THE PENNSYLVANIA STATE UNIVERSITY  
SCHREYER HONORS COLLEGE

DEPARTMENT OF AGRICULTURAL AND BIOLOGICAL ENGINEERING

Analysis of Pollutant Sources and Dynamics in an Urban Stream in Central Pennsylvania

RACHEL STOFANAK  
SPRING 2023

A thesis  
submitted in partial fulfillment  
of the requirements  
for a baccalaureate degree  
in Biological Engineering  
with honors in Biological Engineering

Reviewed and approved\* by the following:

Lauren McPhillips  
Assistant Professor of Civil and Environmental Engineering  
Assistant Professor of Agricultural and Biological Engineering  
Thesis Supervisor

Ali Demirci  
Professor of Agricultural and Biological Engineering  
Honors Adviser

\* Electronic approvals are on file.

## ABSTRACT

Urban streams tend to experience high flows and high loads of pollutants over short periods of time during storm events. When an urban stream is fed by additional sources, such as underground springs, identifying the sources of nitrogen and other pollutants becomes increasingly complex. The purpose of this study is to utilize high-frequency monitoring to determine sources and dynamics of nitrogen and other pollutants in an urban stream with underground springs contributing to flow. High-frequency data on nitrogen, total suspended solids, and total organic carbon was collected every 15 minutes between September 2022 and February 2023, and grab samples were collected during baseflow and storm flow conditions to validate the high-frequency data and find concentrations of additional chemical compounds. Results indicate a dilution pattern for nitrogen during storm events and a flushing pattern for total suspended solids and total organic carbon, indicating that the water from the springs has a higher N concentration which is diluted during storm events, while stormwater has a higher total suspended solids (TSS) and total organic carbon (TOC) concentration that is flushed into the stream during storm events. This information can be used to inform future management recommendations for the surrounding watershed and the areas contributing to the underground springs, as well as potential management interventions along the stream .

## TABLE OF CONTENTS

LIST OF FIGURES.....	iii
LIST OF TABLES.....	iv
ACKNOWLEDGEMENTS.....	v
Chapter 1	
Literature Review.....	1
Water Quality Context .....	1
High-Frequency Data Collection .....	3
Purpose.....	5
Chapter 2	
Methods.....	6
Site Description.....	6
Grab Samples .....	8
Continuous Monitoring.....	9
Storm Event Identification .....	10
Hysteresis Analysis .....	11
Chapter 3	
Results.....	14
Time Series Data.....	14
Grab Sample Analysis.....	19
Hysteresis Analysis .....	21
Analysis of Hysteresis Indices .....	28
Chapter 4	
Discussion and Conclusion.....	32
Possible Pollution Sources .....	32
Comparison to Similar Sites.....	34
Recommendations for Future Work.....	35

## LIST OF FIGURES

- Figure 1: Map of Walnut Run watershed, with the Walnut Springs Park extent highlighted in blue. (a.) Land use within the watershed for Walnut Run is predominantly developed. (b.) Detailed map of sampling locations within Walnut Springs Park..... 7
- Figure 2: Precipitation over the study period (2022-2023), with storms selected for analysis highlighted with a number. Note that storms of a variety of sizes were chosen. .... 11
- Figure 3: Time-series plots of rainfall, temperature, nitrate concentration, TOC concentration, and TSS concentration. No data has been removed, which may result in erroneous or zero values. 16
- Figure 4: Time-series precipitation and concentration data during storm 9. Nitrate concentration experiences a sharp drop and gradual decrease to pre-storm concentration, while TOC and TSS experience a sharp spike and gradual return to baseflow concentrations..... 17
- Figure 5: Nitrate hysteresis for the storm on January 19. Note that the nitrate concentration at the end of the time period is much lower than at the beginning. .... 24
- Figure 6: TOC hysteresis for the storm on January 19. Note that the concentration increases as the water level increases. .... 25
- Figure 7: TSS hysteresis for the storm on January 19. Note that the concentration is the same at the beginning and end of the storm. .... 26
- Figure 8: TOC hysteresis on November 25. Note that concentration during the storm is lower than the initial concentration..... 27
- Figure 9: TSS hysteresis on November 25. Note that concentration before the storm and at the maximum water level are about the same. .... 28

**LIST OF TABLES**

Table 1: Grab sample analysis results during baseflow conditions on September 23. ....	20
Table 2: Grab sample analysis results for storm flow conditions on November 11. ....	21
Table 3: Hysteresis directions for nitrate, TOC, and TSS for each storm. Note that nitrate hysteresis is normally clockwise, while TOC and TSS hysteresis is normally counterclockwise. CW= clockwise; CCW= counter-clockwise; F8= figure eight .....	22
Table 4: Total precipitation and HI and FI for each parameter for all analyzed storms. ....	30

## ACKNOWLEDGEMENTS

This thesis would not have been possible without the support of the people around me. First, I'd like to thank my thesis advisor, Dr. McPhillips, for her valuable guidance and help toward the completion of this thesis. I'd also like to thank my honors adviser, Dr. Demirci, for providing constant support in ensuring that I stay on track. Lastly, to my family and friends, thank you for your support even through my most stressful times this year, even when I wasn't fun to be around.

## **Chapter 1**

### **Literature Review**

#### **Water Quality Context**

Nutrients are known to cause a variety of problems in surface waters. Their impacts include eutrophication, algal blooms, and hypoxia, which can result in fish kills (Bouwman et al., 2013). Common sources of nutrients include wastewater, agricultural runoff, atmospheric deposition, and urban fertilizer application (Kabenge et al., 2016; Walsh et al., 2005; Xu et al., 2019). Wastewater is a particularly common pollution source in urban streams, due to contributions from leaky sewer infrastructure (Aitkenhead-Peterson et al., 2009; Sickman et al., 2007). Agricultural runoff is generally of less concern in an urban stream, but a large watershed can encompass several areas of nonpoint source pollution, including farmland (Boesch et al., 2001). Urban runoff driven by large areas of impervious surface is likely the largest source of pollutants in an urban stream. Pervious urban surfaces like lawns can also be sources of pollution, with higher nitrogen concentrations resulting from fertilizer application (Walsh et al., 2005). Nitrate runoff from residential areas is poorly understood. Groundwater has also been identified as a major source of nutrients, especially in watersheds with a high agricultural or urban development (Robinson, 2015). This is highly dependent upon the source of groundwater entering the stream; groundwater from agricultural land may have a high nitrogen concentration, while urban groundwater may have higher dissolved organic carbon (DOC) from wastewater or residential sources (Sickman et al., 2007). High nutrient concentrations in even small streams can

contribute to impacts downstream as well, if there are not opportunities for removal; for example, nitrate from streams in Iowa contributes to hypoxia in the Gulf of Mexico (Jones et al., 2018). Therefore, understanding the sources of nutrients in small streams is integral to making decisions to improve water quality, both in small watersheds and larger water bodies.

In highly urban watersheds, management decisions are even more important. Urban streams tend to have a flashier hydrograph, greater pollutant concentrations, and lower biodiversity (Meyer et al., 2005). The flashier hydrograph, which results in very high flows during storms, is a result of a combination of increased impervious area and piped stormwater management systems (Dunne & Leopold, 1978). Streams with a high degree of flashiness can degrade quickly during a large storm event, as banks erode and the channel incises, increasing the pollutant load via particle transport (Walsh et al., 2005). Increased pollutant concentrations are also linked with an increase in impervious area in an urban watershed, increasing significantly even with a slight increase in impervious area (Hatt et al., 2004). Specific pollutant increases and impacts are highly depending upon the location and incipient conditions of the watershed and waterway, but greater impervious area results in greater potential for pollutant runoff, and increases in wastewater treatment in a watershed increases risk for sewage contamination in waterways (Horner et al., 1997; Schoonover et al., 2005). Increased pollutant concentration is tied to loss of biodiversity—increased nutrient concentrations can lead to increased algal biomass, which can reduce dissolved oxygen concentrations in waterways and kill more sensitive species (Lee & Bang, 2000). However, in urban streams, high flow variations may disrupt algae growth and show no increase in algae populations, despite increased nutrient concentrations (Hession et al., 2012). Regardless of algae populations, pollution-intolerant species are likely to disappear with increased urbanization: several studies on macroinvertebrates



have shown reduced populations of sensitive species after urbanization (Miltner et al., 2004; Morley & Karr, 2002; Roy et al., 2003). These impacts can be attenuated using smart land management decisions in the watershed, but the water quality of the urban stream must be well understood to inform management.

The Chesapeake Bay watershed is a watershed that spans several US states and includes over 100,000 streams and rivers. Water quality in the Chesapeake Bay has suffered due to the high loads of nutrients and total suspended solids (TSS) received from its many tributaries, both urban and agricultural (Boynton, 2000). Despite efforts to reduce the loads of these pollutants throughout the watershed, water quality has been slow to recover in the bay (Chang et al., 2021). Even in small watersheds, it is necessary to make management decisions to further reduce the nutrient loads reaching the bay.

### **High-Frequency Data Collection**

Storm events can cause disproportionately high pollutant loads to be mobilized in short periods of time. As storms are predicted to increase in frequency and intensity over the coming years it becomes increasingly important to be able to characterize nutrient dynamics throughout a storm. Traditional “grab sampling” provides limited insight into storm dynamics due to the low frequency of the data available. In-situ continuous monitoring provides a clearer picture of changes in nutrient or sediment concentrations based on seasonal, temperature, or storm-based changes with more detail than low-frequency monitoring (Beaulieu et al., 2014; van der Grift et al., 2016). High-frequency monitoring can capture high-resolution data during storms when loads tend to be high and change rapidly and can capture maximum concentrations and loads when

grab samples may not. In-situ monitors also provide the benefit of eliminating any error in capturing or transporting samples that can cause discrepancies in laboratory analyses (Vaughan et al., 2017).

In particular, in-situ optical water quality sensors can provide high-resolution insight into nitrate ( $\text{NO}_3^-$ ), dissolved organic carbon (DOC), and total suspended solids (TSS) concentrations during storm events, all of which are important water quality parameters. DOC tends to be transported from land sources to waterways via storm runoff, or can be generated in situ by vegetation and microbes, and provides information about the total amount of organic matter in the waterway (Volk et al., 2002). Organic matter affects water odor, influences metal pollutant transport, interacts with disinfectants in water to produce harmful byproducts, and can impact overall metabolism and dissolved oxygen (Chow et al., 2007; Ravichandran, 2004). Nitrate is an important nutrient for a healthy ecosystem, but in high concentrations above the biological demand it can cause eutrophication, loss of biodiversity, or increased acidification leading to increased mobility of toxic aluminum (J. P. Baker et al., 1996; Driscoll et al., 1988; Pardo et al., 2011; Smith et al., 1999). TSS provides a glimpse at sediment transport, as well as concentrations of pollutants that sorb to small particles, including nutrients, toxic metals, and organics, all of which are shown to be related to TSS during storm events (Rossi et al., 2005). Therefore, high-frequency monitoring of these specific water quality parameters provides the potential for a greater understanding of water quality dynamics .

Analysis of concentration-discharge relationships collected via high-frequency monitoring in conjunction with precipitation data during a storm event can provide an understanding of how nutrient transport occurs (Bieroza et al., 2018; Duncan et al., 2017). In particular, analysis of hysteresis patterns provides insight into nitrogen dynamics in the stream

(Bowes et al., 2015). Hysteresis patterns occur when the nitrogen concentration is different between the rising and falling parts of the storm. A clockwise relationship, where the nitrogen is higher before the storm peak, indicates that nitrogen sources are nearby and immediately flush the waterway during a storm, and a counterclockwise pattern, where nitrogen is higher after the storm's peak, indicates that the nitrogen sources are farther away or have a longer transport time (Bowes et al., 2005). However, the complexity of nutrient dynamics makes it difficult to draw absolute conclusions about nutrient sources from concentration data alone; hysteresis patterns begin to indicate nitrogen sources, but a clear picture of the sources and dynamics cannot emerge from concentration data alone. Urban streams are particularly difficult to draw conclusions about nutrient sources, as they generally receive very high, flashy flows from a large variety of sources (Leigh et al., 2019).

### **Purpose**

In this study, we focus on an urban stream in central Pennsylvania called Walnut Run. Determining nitrogen sources in Walnut Run is complex: its large urban drainage area, tributaries of two underground springs, and potential leaky wastewater pipes leading to a wastewater treatment plant in an adjacent watershed result in a complex network of potential pollutant sources. Little is known about the stream due to minimal previous research on the area, despite the large volume of scholarship on stormwater in the State College area. This study aims to use a combination of high-frequency monitoring and grab sampling to draw conclusions about nitrogen sources in Walnut Run. This information can then be used to inform management decisions throughout the watershed.

## **Chapter 2 Methods**

### **Site Description**

Walnut Run is in State College in Centre County, Pennsylvania and is located in an urban park, Walnut Springs Park. The area receives an average annual precipitation of 41.53 inches and has an annual average temperature of 51.1°F (NOAA, 2022). The 5.8 km<sup>2</sup> watershed is highly urbanized and receives both direct runoff and runoff from stormwater pipes. The geology in the watershed is largely limestone karst, resulting in the prevalence of groundwater springs. Walnut Run daylights from an underground storm drain on the south end of the park, flowing north, and is joined by several groundwater tributaries a few hundred meters downstream. The stormwater-supplied section of the stream generally has very low flow during baseflow, but receives very high flows during storm events due to the large urban drainage area that was developed prior to current stormwater management guidance. Farther downstream of the springs is a constructed floodplain wetland, a stormwater management practice designed to attenuate high storm flows and reduce pollutant concentrations. There are two inlets to the wetland, a weir and a pipe, both placed so that water enters the wetland primarily during storm flows. Water also enters the wetland through a stormwater pipe from the adjacent residential area. The wetland outlet is located about 100 m downstream of the inlets, conveying water through a pipe with a control box that permits limited outflow to increase wetland retention.

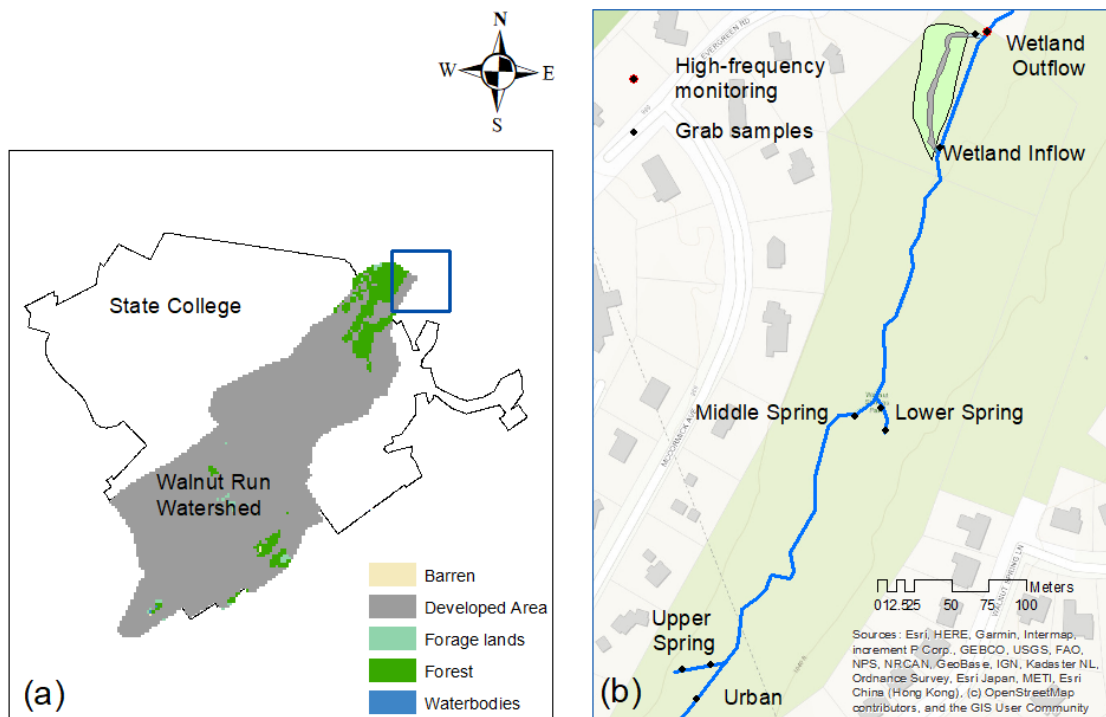


**Figure 1: Map of Walnut Run watershed, with the Walnut Springs Park extent highlighted in blue. (a.) Land use within the watershed for Walnut Run is predominantly developed. (b.) Detailed map of sampling locations within Walnut Springs Park.**

Currently, little is understood about the sources or dynamics of nutrients and sediment entering Walnut Run. Previous research has been conducted on the constructed stormwater wetland's efficiency at pollutant removal and found high concentrations of total dissolved nitrogen during baseflow and high concentrations of total phosphorus and TSS during storm flows, indicating that the springs are likely a source of nitrogen and stormwater is a source of phosphorus and TSS (Fan, 2021). However, no specific information is available about the sources of the pollution within the watershed: there are several potential sources of nitrogen in a

watershed that is highly urbanized with an agricultural history and pipes leading to a wastewater treatment plant in an adjacent watershed.

### **Grab Samples**

Grab samples were collected in the field during both baseflow and storm flow conditions to validate the in-situ sensor data and provide information about additional locations throughout the stream and spring tributaries. During baseflow, samples were collected in the urban stream portion, upstream and downstream sections of each spring, the main stream just after the confluence with the first spring, and just downstream of the wetland outlet, downstream of both springs' confluence with the main stream (Figure 1). During storm events, samples were collected where the stream daylights, further downstream in the urban section before the confluence with the springs, the upstream section of each spring, near the inlet of the wetland, and downstream of the wetland outlet. A total of 14 grab samples were collected during the course of this study: 7 during baseflow conditions and 7 during storm flow conditions. The samples were filtered through a 0.2  $\mu\text{m}$  filter and stored in a refrigerator. A Dionex ion chromatograph was used to analyze the samples for chloride, nitrite, nitrate, sulfate, and phosphate, and a Shimadzu TOC-V and TNM-1 analyzer was used to analyze for total organic carbon and total nitrogen.

### Continuous Monitoring

A TriOS NICO Plus optical water quality sensor was placed downstream of the wetland outlet from September 2022 to March 2023 for the fall, winter, and part of spring seasons. The sensor was housed in a section of PVC piping for protection and was chained to vegetation on the banks to ensure it stayed stationary during high flows. It was powered via a solar panel, and data was downloaded via a USB connection to the control box at an interval of about a month. The spectrophotometer consisted of a xenon flash lamp and four photo diodes, and the nitrate measurements include compensation for turbidity and organic matter. The receiver was cleaned during sampling at regular intervals using an automatic wiper; the recommended wiper life is longer than the scope of this study, so it was not changed during the period of data collection. The PVC casing was cleaned as needed to ensure consistent and representative flow through the sensor. The sensor took samples of nitrate nitrogen (N-NO<sub>3</sub>), nitrogen oxides (NO<sub>x</sub>), chemical oxygen demand (COD), biological oxygen demand (BOD), total organic carbon (TOC), dissolved organic carbon (DOC), turbidity, and TSS at an interval of 15 minutes. Data was downloaded from the field sensor approximately every two weeks.

Conductivity, temperature, and depth data were also measured at a 5 minute interval downstream of the wetland, as well as in the urban section of the stream and in the upper spring, over the same time frame as the TriOS sampler. Conductivity was measured via a conductivity sensor, depth was measured using a pressure transducer connected to an automatic sampler, and temperature was measured via a temperature sensor. Conductivity, temperature, and depth data were collected at the same interval as the data from the TriOS sampler. Precipitation data was acquired from a weather station located nearby on Penn State campus for the study period.

### **Storm Event Identification**

Storms were identified from the precipitation data using two criteria: availability of data and storm intensity. Only storms with both water level and concentration data available for nitrate, TOC, and TSS were included in the analysis, and storms with a variety of total precipitation were chosen, with a focus on larger storms. The beginning of a storm was defined as the time when the water level began to change in response to precipitation, and the end of the storm was defined as the time when the water level returned to pre-storm conditions or when a new storm event begins. In total, 12 rain events over the period of data collection met the criteria for analysis.



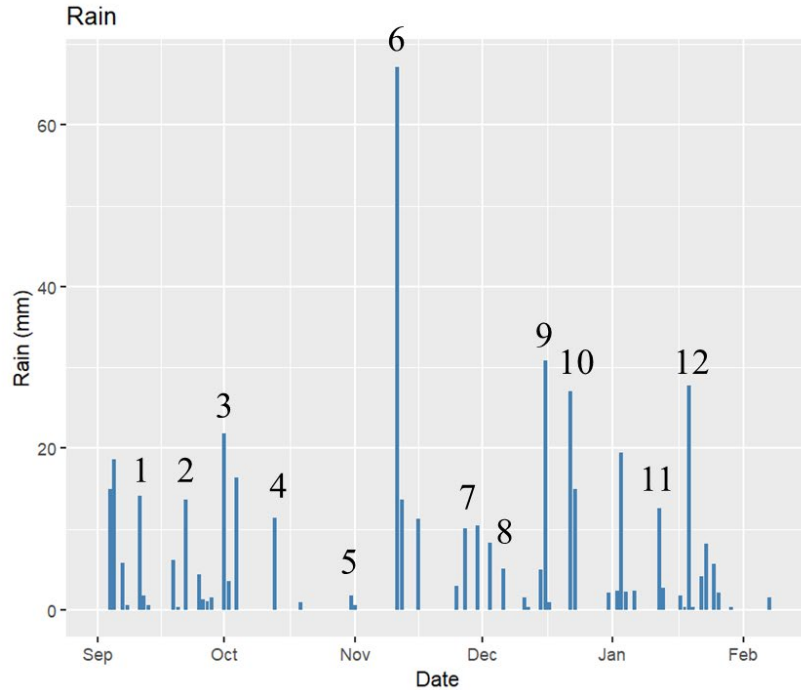


**Figure 2: Precipitation over the study period (2022-2023), with storms selected for analysis highlighted with a number. Note that storms of a variety of sizes were chosen.**

### Hysteresis Analysis

The high-frequency sensor data for concentrations of nitrate, TOC, and TSS, as well as the sensor water level data were utilized to determine detailed hysteresis patterns for the chosen storms. Though discharge is typically compared with concentrations for hysteresis analysis, a water level-discharge relationship has not yet been established for this site, and thus water level is used for hysteresis analysis. First, the water level and concentration data for the 11 storms were graphed in order to visualize the hysteresis patterns and categorize them into clockwise (CW), counterclockwise (CCW), and figure-8 (F8) patterns. The hysteresis indices were then determined using normalized water level and concentration values, as follows:

$$WL_{i,norm} = \frac{WL_i - WL_{min}}{WL_{max} - WL_{min}} \quad (\text{Eqn. 1})$$

$$C_{i,norm} = \frac{C_i - C_{min}}{C_{max} - C_{min}} \quad (\text{Eqn. 2})$$

Where  $WL_i$  and  $C_i$  are the water level and concentration at time step  $i$ ,  $WL_{min}$  and  $C_{min}$  are the minimum water level and concentration in the storm event, and  $WL_{max}$  and  $C_{max}$  are the maximum water level and concentration in the storm event. Using the normalized concentration data, the hysteresis index was calculated using the following:

$$HI = C_{j,rising} - C_{j,falling} \quad (\text{Eqn. 3})$$

Where  $C_{j,rising}$  is the concentration at a certain water level on the rising limb and  $C_{j,falling}$  is the concentration at the same water level on the falling limb. In many cases the concentrations of equal water levels are approximated, as data is not available for equal water levels on the rising and falling limbs. For storms where the falling limb is interrupted by the beginning of another storm event, the hysteresis index calculation included only the portion of the hydrograph before the next storm event begins. This calculation produces an array of individual hysteresis index values for each water level during the storm. The total hysteresis index of the storm was determined to be the mean of this array. The hysteresis index falls between -1 and 1 and provides a numerical indicator of the direction of the hysteresis pattern: a positive value indicates clockwise (CW) hysteresis, indicating that sources are nearby and quickly flush into the waterway, while a negative value indicates counterclockwise (CCW) hysteresis, indicating that

sources travel a distance to reach the waterway or have slower methods of transport. A value close to 0 indicates a figure-8 (F8) pattern. The magnitude of the value indicates the difference between the concentrations on the rising and falling limbs, or the scale of hysteresis, where a 0 value indicates a linear concentration-water level relationship. Flushing index was similarly calculated using the normalized concentration data:

$$FI = C_{peak,norm} - C_{initial,norm} \quad (\text{Eqn. 4})$$

Where  $C_{peak,norm}$  is the normalized concentration at the peak water level in the storm, and  $C_{initial,norm}$  is the normalized concentration at the beginning of the storm before water level begins to change as a response. Flushing index, like hysteresis index, ranges from -1 to 1, with a negative value indicating a dilution pattern on the rising limb of the storm, a positive value indicating a flushing pattern on the rising limb of the storm, and a zero value indicating no relationship between peak water level and concentration. The magnitude of the flushing index indicates the relative amount of solute flushed or diluted. Both the hysteresis index and the flushing index were calculated for all 11 storms for nitrate, TOC, and TSS data.

## **Chapter 3**

### **Results**

#### **Time Series Data**

High-frequency data was collected for 6 months, between September 2022 and February 2023. Precipitation during the study period was consistent with normal central Pennsylvania conditions: one five-year storm was recorded during the study period, as well as one one-year storm, and all other storm events recorded were below the one-year threshold. Every storm event chosen for analysis had a significant impact on nitrate, TOC, and TSS concentrations, proportional to the amount of precipitation. The high-frequency concentration data for nitrate, TOC, and TSS show consistent patterns for concentration during baseflow and rainfall events, but display some erratic data, particularly during the beginning of the monitoring period, as well as some time periods of unavailable data where the concentrations are given as 0. This is likely

due to debris obstructing the sensor receiver, which is more likely to occur at the beginning of the monitoring period in September, when debris in streams with high vegetation cover tends to be high. Storms were chosen to avoid error from missing or erratic sensor data, which may create some bias in that some storms were unable to be analyzed .

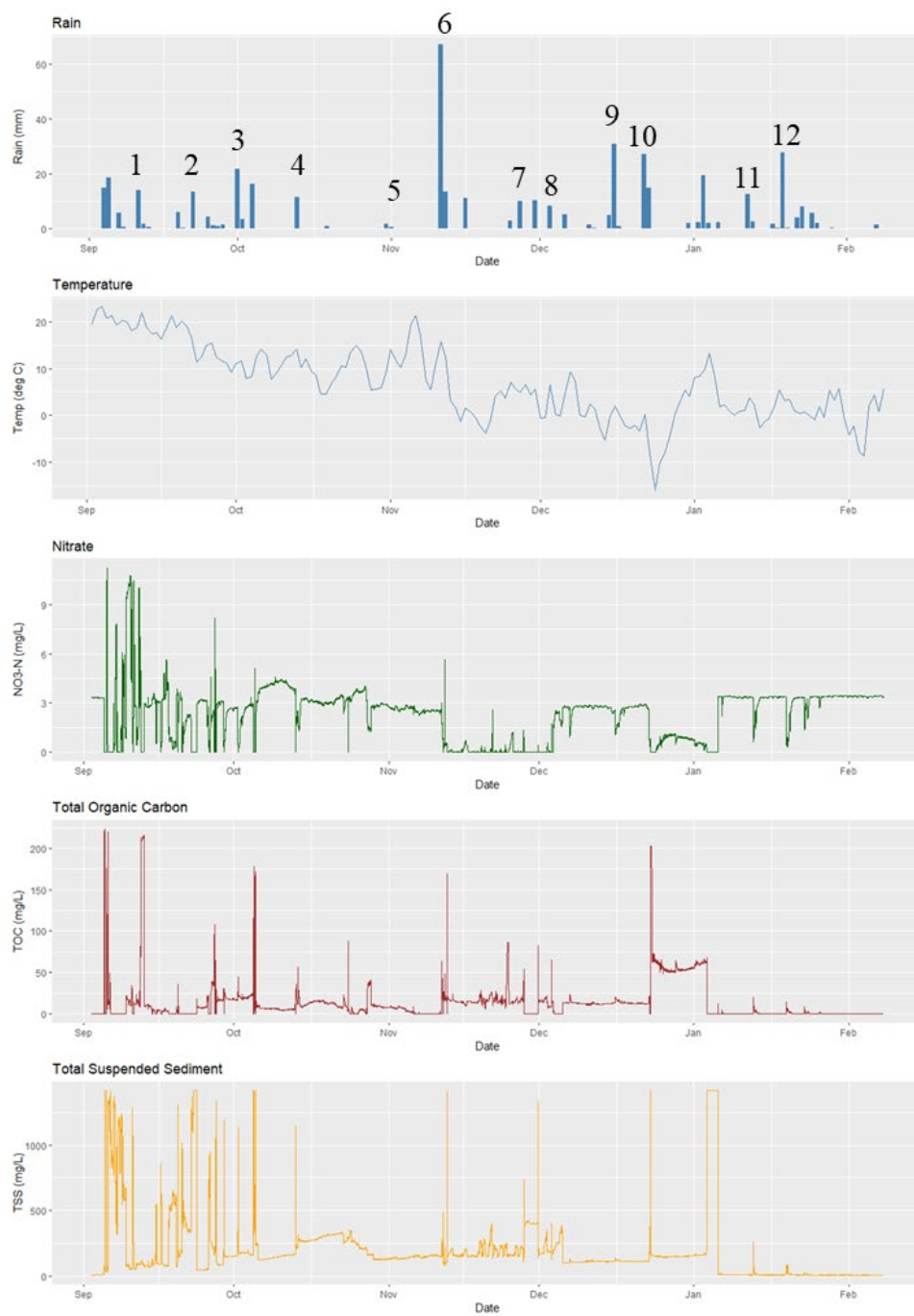


**Figure 3: Time-series plots of rainfall, temperature, nitrate concentration, TOC concentration, and TSS concentration. No data has been removed, which may result in erroneous or zero values.**

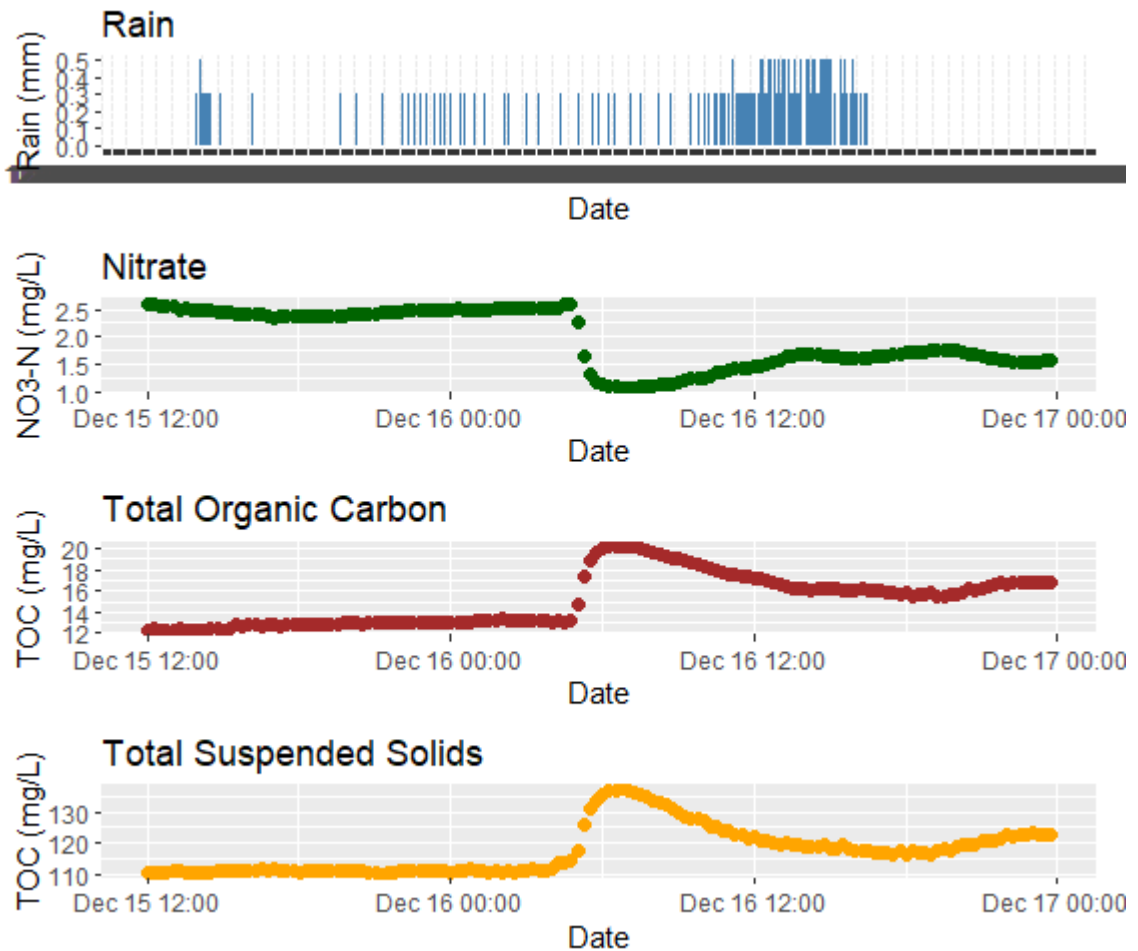


**Figure 4: Time-series precipitation and concentration data during storm 9. Nitrate concentration experiences a sharp drop and gradual decrease to pre-storm concentration, while TOC and TSS experience a sharp spike and gradual return to baseflow concentrations.**

The time series precipitation and concentration data reveal a dilution pattern for nitrate, which decreases in concentration during a storm, as well as a flushing pattern for both TOC and TSS, which increase in concentration during a storm (Figure 3). In many cases, the nitrate dilution pattern mirrors the flushing pattern of TOC and TSS; storm 7 is an exception where a nitrate mobilization pattern occurs, possibly due to the lasting dilution effects of the large storm

6, although TOC and TSS returned quickly to their normal baseflow values rapidly enough to show flushing patterns for storm 7. Another exception is storms 1 and 2, where nitrate concentrations oscillate between unusually low and unusually high. This can be attributed to the stream conditions in September, when a high concentration of organic matter such as fallen leaves tends to be present in the stream, which can significantly affect nitrate concentrations, and the pattern of leaves clogging flow can result in erratic sensor readings. Analysis of high-frequency data for specific storms indicates that dilution and flushing patterns tend to show a very rapid change in concentrations, resulting in sudden drops in nitrate or sudden spikes in TOC and TSS (Figure 4). This indicates very high flows during storm events that drop off quickly, as indicative of a flashy urban stream such as Walnut Run.

The nitrate concentration during the monitoring period ranged from 0 to 11.2694 mg/L, with a mean value of 2.294 mg/L. The minimum of zero likely indicates sensor error, so with the removal of anomalous zero values the mean for nitrate concentration is 2.53 mg/L and the median is 2.78 mg/L. The maximum value exceeds the USEPA limit for drinking water of 10 mg/L, and the mean value, both including and excluding zero values, exceeds the threshold for being considered hypereutrophic (1.5 mg/L). TOC concentrations ranged from 0 to 223.196 mg/L, with a mean of 12.991 mg/L. Excluding anomalous zero values, the mean is 16.36 mg/L and the median is 12.55 mg/L. The mean TOC concentration both including and excluding zero values is high for a stream but remains below the regulation for drinking water (TOC < 25 mg/L). The peak TOC concentration is very high, indicating a high concentration of TOC being flushed into the stream during rain events. The TSS concentration values ranged from 5.270 to 1415.33 mg/L, with a mean of 192.477 mg/L. This indicates a consistently high TSS concentration. Water appears clear when it has a TSS concentration of 20 mg/L, and begins to



appear dirty when the TSS concentration reaches 150 mg/L. The maximum TSS concentration is nearly ten times the threshold for water appearing dirty, indicating that during storm events very high concentrations of TSS are being flushed through the stream from runoff.

### **Grab Sample Analysis**

A total of 14 grab samples were taken and analyzed: one during baseflow conditions (September 23) and one during storm conditions (November 11; storm 6 of the high-frequency analysis). During baseflow conditions, chloride, nitrite-N, sulfate, nitrate-N, TOC, and total nitrogen (TN) show a consistent decrease in concentration as one moves downstream (Table 1). Nitrite and nitrate nitrogen concentrations are very high as the two springs daylight, then decrease significantly as they travel downstream through a vegetated area before joining the main stream. Both nitrite and nitrate nitrogen, as well as total nitrogen, decrease significantly downstream of the wetland, potentially indicating that the wetland has some impact on baseflow nitrogen concentrations, although other factors, such as channel vegetation, may also impact these concentrations. Chloride and sulfate also decrease significantly downstream of the wetland. However, they do not show the same pattern of decreasing in concentration in the two springs as they daylight and travel downstream before joining the main stream—rather, they increase in concentration as they travel toward the main stream. Phosphate was not present in the stream in high enough concentrations to be detected. TOC does not show any consistent pattern of changing from upstream to downstream; it increases as the springs move downstream through the vegetated areas as well as downstream of the wetland, and the highest TOC concentration during baseflow occurs in the urban stormwater section of the stream, indicating that sources of

TOC are likely from the watershed or from internal inputs (e.g. decaying leaves), rather than from groundwater. The urban section of the stream also has the highest concentration of chloride, while it has low concentrations of nitrite and nitrate nitrogen, as well as sulfate and TN. This indicates that the baseflow sources of nitrogen and sulfate are likely groundwater-based rather than from surface sources.

**Table 1: Grab sample analysis results during baseflow conditions on September 23.**

	<b>Chloride</b>	<b>Nitrite-N</b>	<b>Sulfate</b>	<b>Nitrate-N</b>	<b>Phosphate</b>	<b>TOC</b>	<b>TN</b>
<b>Urban</b>	118.54	1.35	6.75	1.41	Negligible	1.28	2.84
<b>Upper Spring</b>	111.29	1.534	8.92	3.32	Negligible	0.37	6.34
<b>Upper Spring 2</b>	113.31	1.44	9.07	3.39	Negligible	0.38	5.93
<b>Mid Spring</b>	113.03	1.60	8.63	2.90	Negligible	0.50	5.73
<b>Lower Spring</b>	108.50	1.57	9.07	3.07	Negligible	0.19	5.61
<b>Lower Spring 2</b>	108.96	1.48	8.97	2.74	Negligible	0.34	4.95
<b>Down Sensor</b>	104.79	1.49	8.39	2.51	Negligible	0.58	4.58

During a storm event, chloride, sulfate, and TOC concentrations were generally higher than baseflow concentrations, while nitrate and nitrite nitrogen and TN concentrations were generally lower than baseflow conditions (Table 2). This further indicates a dilution pattern for nitrogen and a flushing pattern for chloride, sulfate, and TOC. The concentrations that change the most moving downstream are different than in baseflow conditions: in this case, chloride, sulfate, nitrate-nitrogen, and TN follow the pattern of decreasing as water flows downstream from the springs, while nitrite-nitrogen and TOC remain fairly consistent moving downstream. This may indicate that the removal effectiveness of the vegetation and microbial community

changes during high-flow conditions, becoming less effective and removing nitrogen, particularly nitrite. It may also become more effective at removing chloride, although the decrease in chloride concentration may also be due to the spring inputs with lower chloride concentrations. The wetland also shows a particularly effective removal of chloride, although it does not show any significant removal of nitrogen or TOC. Additionally, during storm events the TOC in the urban section of the stream is very high compared to during baseflow conditions, indicating that runoff and stormwater carries high concentrations of TOC into the stream.

**Table 2: Grab sample analysis results for storm flow conditions on November 11.**

	<b>Chloride</b>	<b>Nitrite-N</b>	<b>Sulfate</b>	<b>Nitrate-N</b>	<b>Phosphate</b>	<b>TOC</b>	<b>TN</b>
<b>Daylight</b>	118.41	1.89	26.23	2.01	Negligible	0.54	5.50
<b>Urban</b>	124.38	1.82	25.56	2.15	Negligible	1.80	2.64
<b>Upper Spring</b>	128.00	1.79	27.48	2.74	Negligible	0.41	5.90
<b>Lower Spring</b>	108.66	1.81	28.23	2.78	Negligible	0.21	4.88
<b>Wetland In</b>	123.27	1.88	26.98	2.47	Negligible	0.42	5.34
<b>Wetland Out</b>	108.21	1.91	28.38	2.42	Negligible	0.42	4.90
<b>Down Sensor</b>	115.32	1.94	26.60	1.84	Negligible	0.65	4.12

### **Hysteresis Analysis**

Hysteresis plots were created and hysteresis indices were calculated for all 12 included storms in the study period. Hysteresis plots revealed that in general, nitrate experiences a clockwise hysteresis pattern, where nitrate concentrations are greater on the rising limb than on the falling limb, while TOC and TSS experience a counterclockwise pattern, where the

concentrations of TOC and TSS are higher on the falling limb than on the rising limb (Table 3). However, all of these patterns come with exceptions: nitrate experiences a clockwise pattern for eight out of the 12 storms included, and three others it experiences a figure 8 pattern, with one storm showing a counterclockwise hysteresis pattern for nitrate. TOC experiences a counterclockwise pattern eight of the 12 studied storms, with the other four being figure 8 patterns. TSS also experiences a counterclockwise pattern eight of the 12 storms, with the other four storms being figure 8 patterns. The more unusual or complex hysteresis patterns for all three parameters tended to occur in the fall season or after a major rain event—all of the exceptions to the normal hysteresis patterns occurred between September 19 and December 11, the time of year when leaf litter is the most present in the stream, and all hysteresis patterns in early September and late December or January fit the expected patterns. Thus, it seems likely that the presence of organic debris in the stream has a significant effect on nitrogen, TOC, and TSS dynamics during a storm. In addition, previous rain events likely had an impact on some hysteresis patterns—the storm on November 25 is shortly after the largest storm event in the study period on November 11, which had a total depth of 80.8 mm, and all three parameters show an unusual figure 8 pattern. Therefore, a major storm may have a lasting impact on concentrations of nitrate, TOC, and TSS and affect the dynamics of these parameters during future storms.

**Table 3: Hysteresis directions for nitrate, TOC, and TSS for each storm. Note that nitrate hysteresis is normally clockwise, while TOC and TSS hysteresis is normally counterclockwise. CW= clockwise; CCW= counter-clockwise; F8= figure eight**

Storm	Nitrate Hysteresis	TOC Hysteresis	TSS Hysteresis
-------	--------------------	----------------	----------------

<b>Sept 11 (1)</b>	CW	CCW	CCW
<b>Sept 19 (2)</b>	CW	CCW	CCW
<b>Oct 1 (3)</b>	F8	CCW	F8
<b>Oct 13 (4)</b>	F8	F8	CCW
<b>Oct 31 (5)</b>	CCW	F8	CCW
<b>Nov 11 (6)</b>	CW	F8	F8
<b>Nov 25 (7)</b>	F8	F8	F8
<b>Dec 11 (8)</b>	CW	CCW	F8
<b>Dec 15 (9)</b>	CW	CCW	CCW
<b>Dec 22 (10)</b>	CW	CCW	CCW
<b>Jan 12 (11)</b>	CW	CCW	CCW
<b>Jan 19 (12)</b>	CW	CCW	CCW

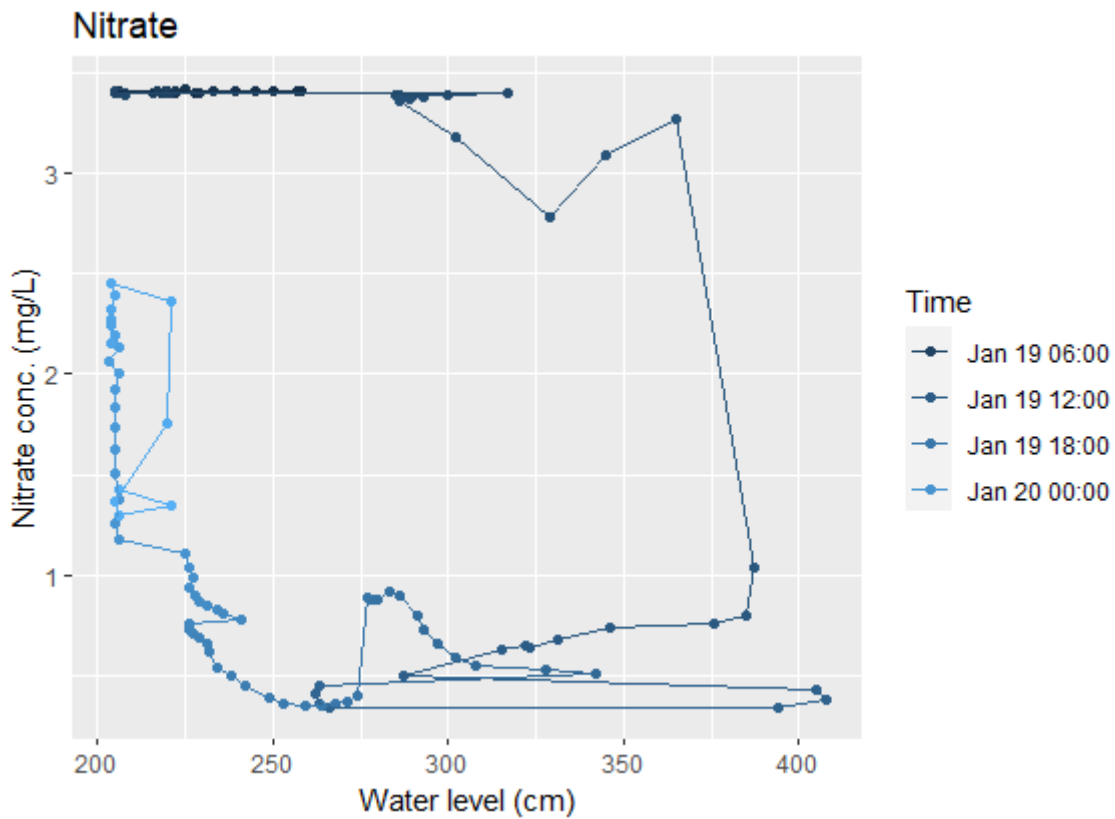


**Figure 5: Nitrate hysteresis for the storm on January 19. Note that the nitrate concentration at the end of the time period is much lower than at the beginning.**

A closer look at the specific hysteresis pattern for specific storms can reveal how nitrate, TOC, and TSS move evolve over the course of a storm. During storm 12 on January 19, nitrate levels are high before the storm begins (about 3.5 mg/L), then are diluted significantly during the storm and never return to pre-storm levels, even as the water level does (Figure 5). This indicates that some nitrate sources near the channel may be diluted and washed out by the high flow during the storm. Similarly, TOC begins at a concentration of 0 mg/L, increases as the water level increases, and returns to a concentration of about 2.5 mg/L as the water level returns to pre-storm levels (Figure 6). The initial TOC value of zero may be due to sensor error, but even

omitting the zero values TOC shows a strong counterclockwise shape and relatively low starting concentration. This may indicate a flushing pattern of TOC where some settles into sediment on the banks and becomes included in baseflow after the storm. TSS shows a different pattern, as the concentration begins and ends at about 12 mg/L at the same water level before and after the storm (Figure 7). This likely indicates that there is a high concentration of TSS in stormwater that flows through the stream but does not settle out during high flows so it has no effect on TSS concentrations in baseflow.

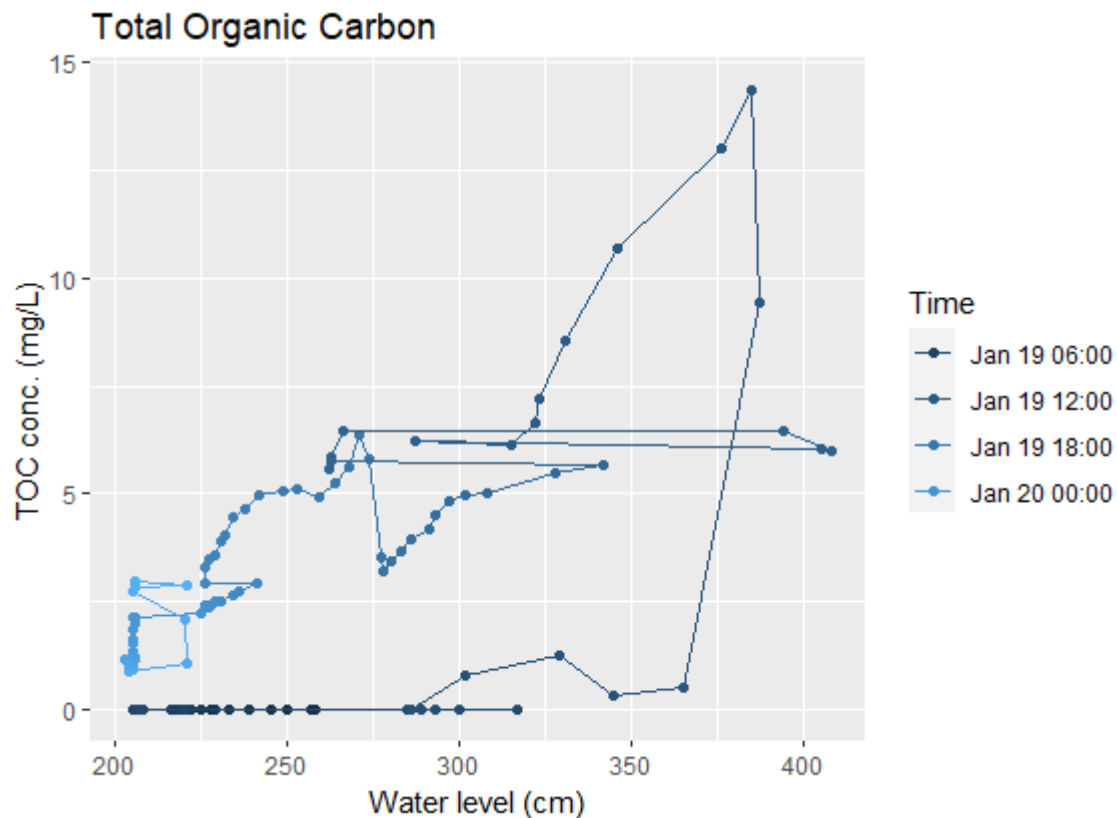


**Figure 6: TOC hysteresis for the storm on January 19. Note that the concentration increases as the water level increases.**

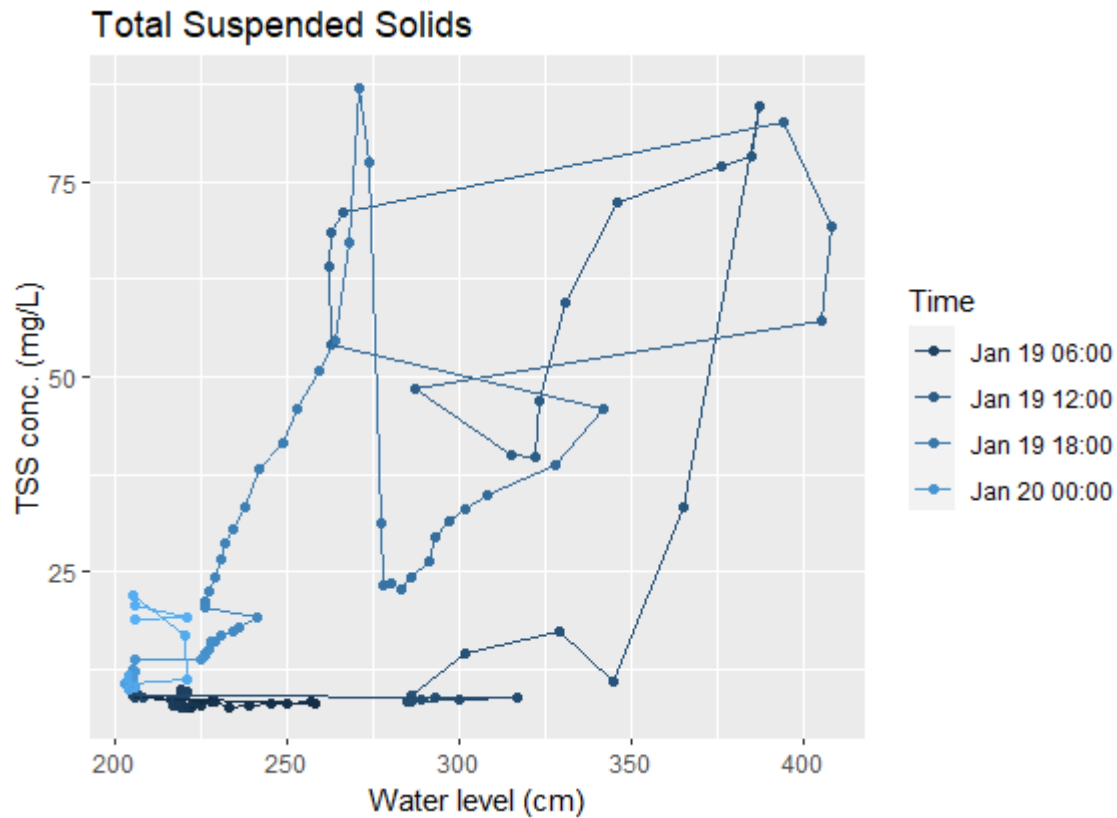


**Figure 7: TSS hysteresis for the storm on January 19. Note that the concentration is the same at the beginning and end of the storm.**

On November 25, the storm impacted by the previous large rain event, nitrate concentrations are near 0 mg/L both before and after the storm, which most likely indicates sensor error throughout the storm. TOC shows a diluting pattern during this storm, with a much lower concentration after the storm (about 15 mg/L) than baseflow before the storm begins (about 20 mg/L) (Figure 9). This likely indicates that the previous storm flushed large volumes of TOC into the channel that settled out and became part of baseflow until the next storm washed



out significant amounts of it. TSS has a similar concentration before and after the storm (about 160 mg/L), and although the concentration varies throughout the storm there is no clear flushing or dilution pattern (Figure 10). This indicates that the previous storm had some impact on TSS in baseflow, but the TSS concentration that remained in the baseflow was similar to the TSS present in stormwater, so an additional storm event had no washing out effect.

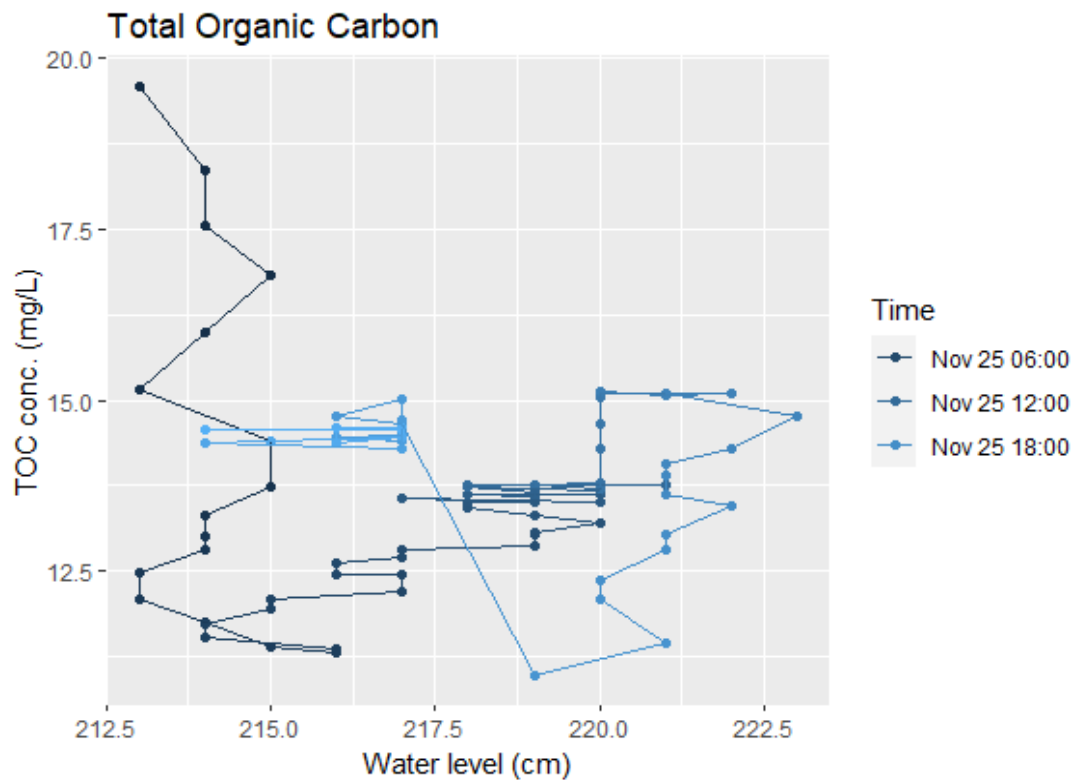


**Figure 8: TOC hysteresis on November 25. Note that concentration during the storm is lower than the initial concentration.**

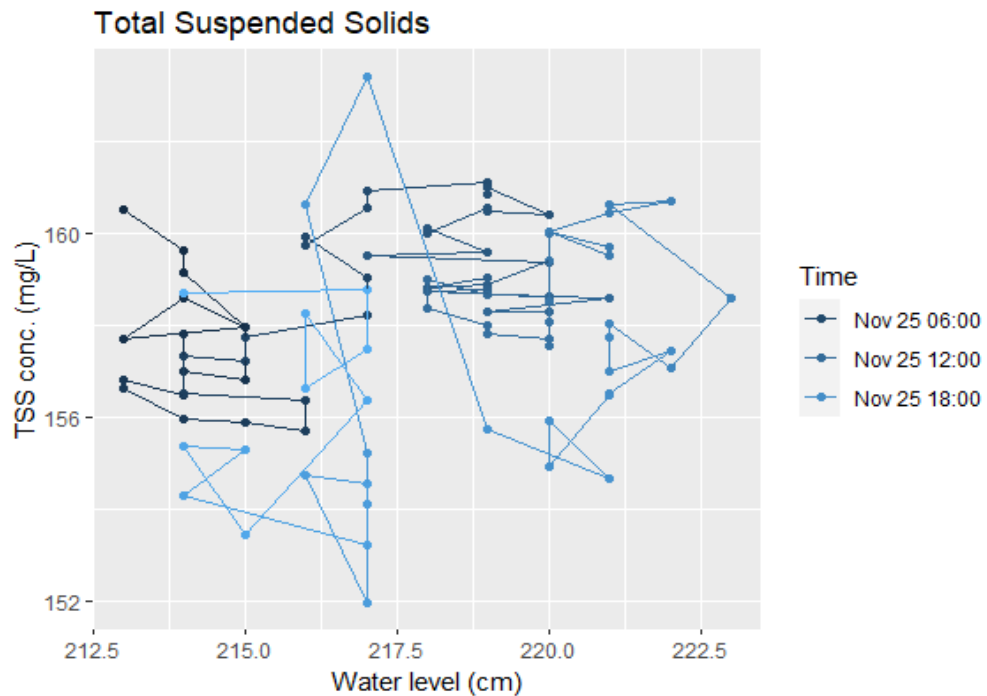


**Figure 9: TSS hysteresis on November 25. Note that concentration before the storm and at the maximum water level are about the same.**

### Analysis of Hysteresis Indices

Calculation of hysteresis indices reveals further insight into nitrate, TOC, and TSS dynamics during storm events. HI for nitrate was generally positive, with a mean of 0.074, which is consistent with the direction of hysteresis generally being clockwise (Table 4). Negative values correlated with storm events where the hysteresis pattern followed a figure 8 or counterclockwise pattern. TOC HI values were generally negative, with a mean of -0.041, which is consistent with the general hysteresis pattern being counterclockwise. Similarly, TSS HI values were generally negative, with a mean of -0.021, as indicated by the counterclockwise hysteresis patterns. FI for nitrate was most often negative, with a mean of -0.082, while FI for TOC and TSS was most often positive, with means of 0.202 and 0.363, respectively. This is

consistent with the dilution pattern of nitrate and the flushing pattern of TOC and TSS observed in the time-series data. The mean HI and FI for nitrate indicate a rapid-connection peak-dilution relationship, indicating that nitrate sources are nearby (i.e. from groundwater/spring baseflow) and are diluted by stormwater. However, the storm events with a negative nitrate HI value instead show a slow-connection peak-dilution pattern (with the exception of the storm on November 25, which shows a slow-connection peak-flushing pattern). This most likely indicates that nitrate sources in stormwater are minimal, but some longer pathways can be activated to flush some nitrate into the stream. No storms exhibited a rapid-connection peak-flushing pattern, indicating that nitrate concentrations increase only after activation of slower pathways. In general, the hysteresis pattern for TOC and TSS was rapid-connection peak-flushing, indicating that nearby and readily available sources of TOC and TSS flush into the stream at the beginning of a storm. There are no exceptions to the flushing pattern, but exceptions to the negative HI show a slow-connection pattern, possibly indicating that rapid connection pathways become exhausted and give way to more distant or slower-activation pathways. In these cases, the HI is positive but very close to 0, so there is likely some contribution from rapid-connection pathways, but slow-connection pathways dominate. This also tends to occur during events with higher-than-average rainfall or unusually low rainfall, which may indicate that a large storm exhausts the rapid-connection pathways to activate the slow-connection pathways or that smaller rain events are more likely to activate the slow-connection pathways.

**Table 4: Total precipitation and HI and FI for each parameter for all analyzed storms.**

<b>Storm</b>	<b>Total Precip (mm)</b>	<b>HI (NO3)</b>	<b>FI (NO3)</b>	<b>HI (TOC)</b>	<b>FI (TOC)</b>	<b>HI (TSS)</b>	<b>FI (TSS)</b>
<b>Sept 11 (1)</b>	14.1	0.15	0.73	-0.018	0.11	0.0049	0.0013
<b>Sept 19 (2)</b>	6.5	0.069	0.045	-0.033	0.13	-0.058	0.88
<b>Oct 1 (3)</b>	23.6	0.083	0.0023	-0.0091	0.124	-0.012	0.70
<b>Oct 13 (4)</b>	11.4	0.16	0.0050	-0.080	0.23	-0.065	0.70
<b>Oct 31 (5)</b>	2.4	-0.016	0.0026	0.0018	0.0097	0.0018	0.0012
<b>Nov 11 (6)</b>	80.8	-0.11	0.28	0.035	0.76	-0.0050	0.90
<b>Nov 25 (7)</b>	2.9	-0.021	0.11	-0.0022	0	0.0013	0.0020
<b>Dec 11 (8)</b>	1.8	0.0039	0.0035	-0.0028	0.016	0.00083	0.0012
<b>Dec 15 (9)</b>	36.7	0.016	0.015	0.0012	0.036	0.00058	0.019
<b>Dec 22 (10)</b>	42	.20	0	-0.35	0.86	-0.091	0.92
<b>Jan 12 (11)</b>	15.3	0.12	0.0016	-0.016	0.088	-0.012	0.18
<b>Jan 19 (12)</b>	28.1	0.24	0.0020	-0.018	0.064	-0.017	0.056

Total storm precipitation is generally correlated with greater impacts on concentrations—during the largest storm during the time period, on November 11, all parameters experience their maximum FI (or minimum in the case of nitrate, indicating the greatest dilution effect), as well as a maximum or nearly maximum HI. Events with a large HI that does not correlate with a large rainfall event are most likely affected by antecedent conditions: HI tends to be larger, particularly for TOC and TSS, after a period of dry conditions. In two cases FI is equal to zero, once for nitrate and once for TOC, which may be due to a combination of antecedent conditions and flushing pathways that result in no net change in concentration throughout the storm event. In these cases, HI is not equal to zero, indicating some correlation between concentration and water level on the rising and falling limbs of the storm, although the concentration is the same at the baseflow water level and the maximum water level.

## Chapter 4

### Discussion and Conclusion

#### Possible Pollution Sources

The dilution pattern of nitrate that is clear from the time series data and hysteresis analysis, as well as the grab sample analysis of nitrate, nitrite, and TN, indicates a high contribution of nitrate from the two groundwater springs that join Walnut Run in the park and provide the majority of its baseflow. In addition, hysteresis analysis of nitrate indicates that nitrate sources are nearby the stream and do not follow delayed pathways entering the stream. It is common for underground springs to have high nitrate concentrations, as common nitrate removal mechanisms, such as wetland vegetation, cannot occur in an underground spring with sunlight unavailability (Beaulieu et al., 2014). This indicates that the sources of nitrate are most likely to be from readily available sources that often leach into groundwater, such as agricultural sources, urban fertilizers, or wastewater leaks, all of which are common wastewater nitrate contaminants in Pennsylvania (Spalding & Exner, 1993). The Walnut Run watershed is largely urban but has a legacy of agricultural land use that may act as a source of nitrate, and pipes leading to the wastewater treatment plant in the adjacent watershed may leak. Both wastewater effluent and urban fertilizer are plausible sources: wastewater leaks tend to have nitrate concentrations around 25 mg/L, resulting in groundwater concentrations between 10 and 30 mg/L, and urban fertilizer tends to have nitrate concentrations of 1-5 mg/L (Wakida & Lerner, 2005). Nitrogen concentrations over the time period had a mean value of 2.3 mg/L and a maximum value of 11.3 mg/L. Legacy agricultural nitrate is also a plausible explanation, as

studies have shown agriculture to lead to high levels of nitrate accumulation in groundwater and that agricultural nitrate has a long residence time that can affect groundwater concentrations for several years (Ilampooranan et al., 2022; Stets et al., 2020). It is difficult to draw definitive conclusions about nitrate sources, but further specific analysis of nitrogen dynamics could further narrow down the potential sources.

The flushing pattern of TOC, along with the counterclockwise hysteresis pattern, indicate that the sources of TOC in the stream enter the stream via stormwater runoff, and have a short pathway to reach the stream. Atmospheric TOC is a possible source of TOC in stormwater, as rain plays an important role in carbon cycling to surface waters (Willey et al., 2000). Stormwater management practices, such as stormwater ponds, can also contribute to TOC concentrations in streams, as aquatic life such as algae can be abundant and convert other nutrient inputs into organic carbon (Kalev et al., 2021). Urban streams such as Walnut Run are more likely to experience higher TOC concentrations due to the lack of carbon sinks present in urban areas, such as vegetated areas. TOC is also likely to be affected seasonally by organic debris in the stream: the presence of leaf litter in the stream in fall can increase TOC retention and release organic matter that contribute to higher TOC concentrations (Mulholland & Hill, 1997).

Like TOC, TSS time series and hysteresis analysis shows a rapid-release flushing pattern, indicating that sources enter the stream via stormwater runoff from readily available sources. Sources of TSS in stormwater runoff from urban areas are well documented; they include anthropogenic activity, such as construction, increases in soil erosion potential, and residential litter (Rossi et al., 2013). TSS in runoff tends to be the greatest from residential areas, a land use that takes up much of Walnut Run's watershed. As a largely urban watershed with a

flashy hydrograph, Walnut Run does not experience significant sediment buildup, as TSS concentration during baseflow is generally very low. As a result, TSS that wash into Walnut Run from the surrounding areas due to urbanization and residential land use likely flow downstream and cause sedimentation in larger downstream surface waters; minimizing the TSS that reach Walnut Run would likely have little impact on water quality in Walnut Run during baseflow, but may have significant effects on downstream water quality. Additional sources of TSS may be erosion of the banks of Walnut Run, driven by its high velocity stormflows (Percich et al., 2022).

### **Comparison to Similar Sites**

Hysteresis analysis is an emerging method for determining pollutant dynamics in streams in watersheds of all land uses. Liu et al., in a review of hysteresis analysis methods, concluded that hysteresis analysis can provide useful insight into complex nutrient dynamics, but cannot characterize these dynamics on its own (Liu et al., 2021). In an analysis of an urbanized watershed in North Carolina, Rose determined that urbanization leads to complex processes that affect pollutant concentrations in stormwater, groundwater, and soil, and hysteresis loops provide some insight into the comparative pollutant concentrations (Rose, 2003). This provides information for drawing conclusions about sources of nitrogen: along with information about the land use in the watershed, it is possible to narrow down the possible sources of pollutants. However, these dynamics can be very complex, and it is difficult to draw clear definitive conclusions about the processes occurring in the soil and water with concentration-discharge information alone. Evans et al., however, was able to trace high nitrate concentrations in a New York stream to runoff contact with soil high in organic matter (Evans et al., 1999). Husic et al.



analyzed sediment hysteresis in rural and urban streams in Kansas, concluding that the presence of wastewater treatment facilities can also increase prevalence of TSS in an urban stream (Husic et al., 2023). Zhang et al. performed a hysteresis analysis using high-frequency sensing in a karst catchment, concluding that the rapid infiltration in karst soil results in rapid mobilization of soil nitrate into groundwater (Zhang et al., 2021). Several other analyses have determined that hysteresis patterns are dominated by a single shape, indicating consistent pollutant sources across seasonal changes, although other analyses have found inconsistent hysteresis patterns across seasons (E. B. Baker & Showers, 2019; Jacobs et al., 2018). In all, it is difficult to draw definitive conclusions about pollutant sources, but hysteresis patterns provide significant insight into complex dynamics occurring in a watershed.

### **Recommendations for Future Work**

Hysteresis analysis provided significant insight into potential pollutant sources in Walnut Run watershed, but it is difficult to draw clear conclusions about sources of nitrate, TOC, and TSS in a watershed with many potential sources. High-frequency sensing can be further utilized to better characterize the dynamics, particularly with seasonal variation if data is collected throughout the year, or multiple years with variation in hydrologic conditions. Low-frequency data collection could also be used to gather further insight into pollutant dynamics throughout the stream with additional sampling during baseflow and storm event periods, particularly a variety of storm sizes and antecedent conditions. Additionally, sources of nitrate can be best characterized by isotopic analysis of stream samples, as the presence of isotopes of  $\text{NO}_3$  can lead to better conclusions about nitrate sources than concentration-discharge relationships alone. Last,

groundwater analysis can provide better insight into the sources of the springs and inform land management decisions throughout the watershed to minimize nitrate leaching into groundwater, as well as TOC and TSS concentrations in runoff.

## BIBLIOGRAPHY

- Aitkenhead-Peterson, J. A., Steele, M. K., Nahar, N., & Santhy, K. (2009). Dissolved organic carbon and nitrogen in urban and rural watersheds of south-central Texas: land use and land management influences. *Biogeochemistry*, *96*(1), 119–129.  
<https://doi.org/10.1007/s10533-009-9348-2>
- Baker, E. B., & Showers, W. J. (2019). Hysteresis analysis of nitrate dynamics in the Neuse River, NC. *Science of The Total Environment*, *652*, 889–899.  
<https://doi.org/10.1016/j.scitotenv.2018.10.254>
- Baker, J. P., Van Sickle, J., Gagen, C. J., DeWalle, D. R., Sharpe, W. E., Carline, R. F., et al. (1996). Episodic Acidification of Small Streams in the Northeastern United States: Effects on Fish Populations. *Ecological Applications*, *6*(2), 422–437.  
<https://doi.org/10.2307/2269380>
- Beaulieu, J. J., Mayer, P. M., Kaushal, S. S., Pennino, M. J., Arango, C. P., Balz, D. A., et al. (2014). Effects of urban stream burial on organic matter dynamics and reach scale nitrate retention. *Biogeochemistry*, *121*(1), 107–126. <https://doi.org/10.1007/s10533-014-9971-4>
- Bieroza, M. Z., Heathwaite, A. L., Bechmann, M., Kyllmar, K., & Jordan, P. (2018). The concentration-discharge slope as a tool for water quality management. *Science of the Total Environment*, *630*, 738–749. <https://doi.org/10.1016/j.scitotenv.2018.02.256>
- Boesch, D. F., Brinsfield, R. B., & Magnien, R. E. (2001). Chesapeake Bay Eutrophication: Scientific Understanding, Ecosystem Restoration, and Challenges for Agriculture. *Journal of Environmental Quality*, *30*(2), 303–320.  
<https://doi.org/10.2134/jeq2001.302303x>

- Bouwman, A. F., Bierkens, M. F. P., Griffioen, J., Hefting, M. M., Middelburg, J. J., Middelkoop, H., & Slomp, C. P. (2013). Nutrient dynamics, transfer and retention along the aquatic continuum from land to ocean: towards integration of ecological and biogeochemical models. *Biogeosciences*, *10*(1), 1–22. <https://doi.org/10.5194/bg-10-1-2013>
- Bowes, M. J., House, W. A., Hodgkinson, R. A., & Leach, D. V. (2005). Phosphorus-discharge hysteresis during storm events along a river catchment: the River Swale, UK. *Water Research*, *39*(5), 751–762. <https://doi.org/10.1016/j.watres.2004.11.027>
- Boynton, W. R. (2000). Impact of nutrient inflows on Chesapeake Bay. In A. N. Sharpley (Ed.), *Agriculture and Phosphorus Management: The Chesapeake Bay* (pp. 23–40). Boca Raton: Lewis Publishers Inc. Retrieved from <https://www.webofscience.com/wos/woscc/full-record/WOS:000085842300004>
- Chang, S. Y., Zhang, Q., Byrnes, D. K., Basu, N. B., & Van Meter, K. J. (2021). Chesapeake legacies: the importance of legacy nitrogen to improving Chesapeake Bay water quality. *Environmental Research Letters*, *16*(8), 085002. <https://doi.org/10.1088/1748-9326/ac0d7b>
- Chow, A. T., Dahlgren, R. A., & Harrison, J. A. (2007). Watershed Sources of Disinfection Byproduct Precursors in the Sacramento and San Joaquin Rivers, California. *Environmental Science & Technology*, *41*(22), 7645–7652. <https://doi.org/10.1021/es070621t>
- Driscoll, C. T., Fuller, R. D., & Simone, D. M. (1988). Longitudinal Variations in Trace Metal Concentrations in a Northern Forested Ecosystem. *Journal of Environmental Quality*, *17*(1), 101–107. <https://doi.org/10.2134/jeq1988.00472425001700010015x>

- Duncan, J. M., Welty, C., Kemper, J. T., Groffman, P. M., & Band, L. E. (2017). Dynamics of nitrate concentration-discharge patterns in an urban watershed. *Water Resources Research*, 53(8), 7349–7365. <https://doi.org/10.1002/2017WR020500>
- Dunne, T., & Leopold, L. B. (1978). *Water in Environmental Planning*. Macmillan.
- Evans, C., Davies, T. D., & Murdoch, P. S. (1999). Component flow processes at four streams in the Catskill Mountains, New York, analysed using episodic concentration/discharge relationships. *Hydrological Processes*, 13(4), 563–575. [https://doi.org/10.1002/\(SICI\)1099-1085\(199903\)13:4<563::AID-HYP711>3.0.CO;2-N](https://doi.org/10.1002/(SICI)1099-1085(199903)13:4<563::AID-HYP711>3.0.CO;2-N)
- Fan, L. (n.d.). Environmental Engineering.
- van der Grift, B., Broers, H. P., Berendrecht, W., Rozemeijer, J., Oste, L., & Griffioen, J. (2016). High-frequency monitoring reveals nutrient sources and transport processes in an agriculture-dominated lowland water system. *Hydrology and Earth System Sciences*, 20(5), 1851–1868. <https://doi.org/10.5194/hess-20-1851-2016>
- Hatt, B. E., Fletcher, T. D., Walsh, C. J., & Taylor, S. L. (2004). The Influence of Urban Density and Drainage Infrastructure on the Concentrations and Loads of Pollutants in Small Streams. *Environmental Management*, 34(1), 112–124. <https://doi.org/10.1007/s00267-004-0221-8>
- Hession, W. C., Johnson, T. E., Charles, D. F., Horwitz, R. J., Kreeger, D. A., Marshall, B. D., et al. (2012). Ecological Benefits of Riparian Reforestation in Urban Watersheds, 373–382. [https://doi.org/10.1061/40695\(2004\)9](https://doi.org/10.1061/40695(2004)9)
- Horner, R. R., Booth, D. B., Azous, A., & May, C. W. (1997). Watershed Determinants of Ecosystem Functioning (pp. 251–274). Presented at the Effects of Watershed

- Development and Management on Aquatic Ecosystems, ASCE. Retrieved from <https://cedb.asce.org/CEDBsearch/record.jsp?dockkey=0104864>
- Husic, A., Fox, J. F., Clare, E., Mahoney, T., & Zarnaghsh, A. (2023). Nitrate Hysteresis as a Tool for Revealing Storm-Event Dynamics and Improving Water Quality Model Performance. *Water Resources Research*, *59*(1), e2022WR033180. <https://doi.org/10.1029/2022WR033180>
- Ilampooranan, I., Meter, K. J. V., & Basu, N. B. (2022). Intensive agriculture, nitrogen legacies, and water quality: intersections and implications. *Environmental Research Letters*, *17*(3), 035006. <https://doi.org/10.1088/1748-9326/ac55b5>
- Jacobs, S. R., Weeser, B., Guzha, A. C., Rufino, M. C., Butterbach-Bahl, K., Windhorst, D., & Breuer, L. (2018). Using High-Resolution Data to Assess Land Use Impact on Nitrate Dynamics in East African Tropical Montane Catchments. *Water Resources Research*, *54*(3), 1812–1830. <https://doi.org/10.1002/2017WR021592>
- Jones, C. S., Nielsen, J. K., Schilling, K. E., & Weber, L. J. (2018). Iowa stream nitrate and the Gulf of Mexico. *PLOS ONE*, *13*(4), e0195930. <https://doi.org/10.1371/journal.pone.0195930>
- Kabenge, M., Wang, H., & Li, F. (2016). Urban eutrophication and its spurring conditions in the Murchison Bay of Lake Victoria. *Environmental Science and Pollution Research*, *23*(1), 234–241. <https://doi.org/10.1007/s11356-015-5675-0>
- Kalev, S., Duan, S., & Toor, G. S. (2021). Enriched dissolved organic carbon export from a residential stormwater pond. *Science of The Total Environment*, *751*, 141773. <https://doi.org/10.1016/j.scitotenv.2020.141773>

- Lee, J. H., & Bang, K. W. (2000). Characterization of urban stormwater runoff. *Water Research*, 34(6), 1773–1780. [https://doi.org/10.1016/S0043-1354\(99\)00325-5](https://doi.org/10.1016/S0043-1354(99)00325-5)
- Leigh, C., Kandanaarachchi, S., McGree, J. M., Hyndman, R. J., Alsibai, O., Mengersen, K., & Peterson, E. E. (2019). Predicting sediment and nutrient concentrations from high-frequency water-quality data. *Plos One*, 14(8), e0215503. <https://doi.org/10.1371/journal.pone.0215503>
- Liu, W., Birgand, F., Tian, S., & Chen, C. (2021). Event-scale hysteresis metrics to reveal processes and mechanisms controlling constituent export from watersheds: A review☆. *Water Research*, 200, 117254. <https://doi.org/10.1016/j.watres.2021.117254>
- Meyer, J. L., Paul, M. J., & Taulbee, W. K. (2005). Stream ecosystem function in urbanizing landscapes. *Journal of the North American Benthological Society*, 24(3), 602–612. <https://doi.org/10.1899/04-021.1>
- Miltner, R. J., White, D., & Yoder, C. (2004). The biotic integrity of streams in urban and suburbanizing landscapes. *Landscape and Urban Planning*, 69(1), 87–100. <https://doi.org/10.1016/j.landurbplan.2003.10.032>
- Morley, S. A., & Karr, J. R. (2002). Assessing and Restoring the Health of Urban Streams in the Puget Sound Basin. *Conservation Biology*, 16(6), 1498–1509. <https://doi.org/10.1046/j.1523-1739.2002.01067.x>
- Mulholland, P. J., & Hill, W. R. (1997). Seasonal patterns in streamwater nutrient and dissolved organic carbon concentrations: Separating catchment flow path and in-stream effects. *Water Resources Research*, 33(6), 1297–1306. <https://doi.org/10.1029/97WR00490>

NOAA NCEI U.S. Climate Normals Quick Access. (n.d.). Retrieved March 19, 2023, from

<https://www.ncei.noaa.gov/access/us-climate-normals/#dataset=normals-monthly&timeframe=30&station=USC00368449>

Pardo, L. H., Fenn, M. E., Goodale, C. L., Geiser, L. H., Driscoll, C. T., Allen, E. B., et al.

(2011). Effects of nitrogen deposition and empirical nitrogen critical loads for ecoregions of the United States. *Ecological Applications*, *21*(8), 3049–3082.

<https://doi.org/10.1890/10-2341.1>

Percich, A., Husic, A., & Ketterer, M. E. (2022). Plutonium Isotopes: An Effective Tool for

Fluvial Sediment Sourcing in Urbanized Catchments. *Geophysical Research Letters*, *49*(2), e2021GL094497. <https://doi.org/10.1029/2021GL094497>

Ravichandran, M. (2004). Interactions between mercury and dissolved organic matter—a review.

*Chemosphere*, *55*(3), 319–331. <https://doi.org/10.1016/j.chemosphere.2003.11.011>

Robinson, C. (2015). Review on groundwater as a source of nutrients to the Great Lakes and their tributaries. *Journal of Great Lakes Research*, *41*(4), 941–950.

<https://doi.org/10.1016/j.jglr.2015.08.001>

Rose, S. (2003). Comparative solute–discharge hysteresis analysis for an urbanized and a

‘control basin’ in the Georgia (USA) Piedmont. *Journal of Hydrology*, *284*(1), 45–56.

<https://doi.org/10.1016/j.jhydrol.2003.07.001>

Rossi, L., Krejci, V., Rauch, W., Kreikenbaum, S., Fankhauser, R., & Gujer, W. (2005).

Stochastic modeling of total suspended solids (TSS) in urban areas during rain events.

*Water Research*, *39*(17), 4188–4196. <https://doi.org/10.1016/j.watres.2005.07.041>



- Rossi, L., Chèvre, N., Fankhauser, R., Margot, J., Curdy, R., Babut, M., & Barry, D. A. (2013). Sediment contamination assessment in urban areas based on total suspended solids. *Water Research*, 47(1), 339–350. <https://doi.org/10.1016/j.watres.2012.10.011>
- Roy, A. H., Rosemond, A. D., Paul, M. J., Leigh, D. S., & Wallace, J. B. (2003). Stream macroinvertebrate response to catchment urbanisation (Georgia, U.S.A.). *Freshwater Biology*, 48(2), 329–346. <https://doi.org/10.1046/j.1365-2427.2003.00979.x>
- Schoonover, J. E., Lockaby, B. G., & Pan, S. (2005). Changes in chemical and physical properties of stream water across an urban-rural gradient in western Georgia. *Urban Ecosystems*, 8(1), 107–124. <https://doi.org/10.1007/s11252-005-1422-5>
- Sickman, J. O., Zanolli, M. J., & Mann, H. L. (2007). Effects of Urbanization on Organic Carbon Loads in the Sacramento River, California. *Water Resources Research*, 43(11). <https://doi.org/10.1029/2007WR005954>
- Smith, V. H., Tilman, G. D., & Nekola, J. C. (1999). Eutrophication: impacts of excess nutrient inputs on freshwater, marine, and terrestrial ecosystems. *Environmental Pollution*, 100(1), 179–196. [https://doi.org/10.1016/S0269-7491\(99\)00091-3](https://doi.org/10.1016/S0269-7491(99)00091-3)
- Spalding, R. F., & Exner, M. E. (1993). Occurrence of Nitrate in Groundwater—A Review. *Journal of Environmental Quality*, 22(3), 392–402. <https://doi.org/10.2134/jeq1993.00472425002200030002x>
- Stets, E. G., Sprague, L. A., Oelsner, G. P., Johnson, H. M., Murphy, J. C., Ryberg, K., et al. (2020). Landscape Drivers of Dynamic Change in Water Quality of U.S. Rivers. *Environmental Science & Technology*, 54(7), 4336–4343. <https://doi.org/10.1021/acs.est.9b05344>

- Vaughan, M. C. H., Bowden, W. B., Shanley, J. B., Vermilyea, A., Sleeper, R., Gold, A. J., et al. (2017). High-frequency dissolved organic carbon and nitrate measurements reveal differences in storm hysteresis and loading in relation to land cover and seasonality. *Water Resources Research*, 53(7), 5345–5363. <https://doi.org/10.1002/2017WR020491>
- Volk, C., Wood, L., Johnson, B., Robinson, J., Wei Zhu, H., & Kaplan, L. (2002). Monitoring dissolved organic carbon in surface and drinking waters. *Journal of Environmental Monitoring*, 4(1), 43–47. <https://doi.org/10.1039/B107768F>
- Wakida, F. T., & Lerner, D. N. (2005). Non-agricultural sources of groundwater nitrate: a review and case study. *Water Research*, 39(1), 3–16. <https://doi.org/10.1016/j.watres.2004.07.026>
- Walsh, C. J., Roy, A. H., Feminella, J. W., Cottingham, P. D., Groffman, P. M., & Morgan, R. P. (2005). The urban stream syndrome: current knowledge and the search for a cure. *Journal of the North American Benthological Society*, 24(3), 706–723. <https://doi.org/10.1899/04-028.1>
- Willey, J. D., Kieber, R. J., Eyman, M. S., & Avery Jr., G. B. (2000). Rainwater dissolved organic carbon: Concentrations and global flux. *Global Biogeochemical Cycles*, 14(1), 139–148. <https://doi.org/10.1029/1999GB900036>
- Xu, J., Jin, G., Tang, H., Mo, Y., Wang, Y.-G., & Li, L. (2019). Response of water quality to land use and sewage outfalls in different seasons. *Science of the Total Environment*, 696. <https://doi.org/10.1016/j.scitotenv.2019.134014>
- Zhang, Z., Chen, X., Li, S., Yue, F., Cheng, Q., Peng, T., & Soulsby, C. (2021). Linking nitrate dynamics to water age in underground conduit flows in a karst catchment. *Journal of Hydrology*, 596, 125699. <https://doi.org/10.1016/j.jhydrol.2020.125699>

## ACADEMIC VITA

### Rachel Stofanak

#### **Education:**

---

Bachelor of Science in Biological Engineering, Natural Resources Engineering option

The Pennsylvania State University

Schreyer Honors College

Graduation Date: May 2023

#### **Skills:**

---

SolidWorks, ArcGIS, Microsoft Excel, MATLAB, Plant Identification, Surveying (Laser Level and TotalStation), R, HEC-RAS (beginner)

#### **Experience:**

---

Undergraduate Thesis—*Penn State Department of Civil Engineering* May 2022-Present

- Completed a literature review of previous work on similar topics.
- Collected and analyzed data involving nitrogen dynamics in an urban stream.
- Completed water quality data analysis.

Teaching Assistant—*Penn State Department of Biological Engineering* May 2022-Present

- Provided feedback to over 40 students with technical and career writing assignments.
- Worked professionally with students and staff.
- Assisted faculty with grading and organizing assignments.

Student Worker—*Penn State Dairy Barn* May-August 2022

- Coordinated smooth operation of milking over 200 cows per day.
- Performed daily operations independently.
- Trained other workers in job duties.

Pathways Intern—*Natural Resources Conservation Service* May-August 2021

- Worked with two farmers to develop conservation plans for their land.
- Surveyed and monitored erosion in landscapes.
- Designed conservation practices for sustainable water and nutrient management.

Study Group Facilitator—*Penn State Women in Engineering Program* January-May 2021

- Facilitated weekly discussions around problem-solving applied to introductory physics.
- Assisted other students with understanding basic physics concepts.
- Mentored ten underclass students.

#### **Involvement:**

---

- Gender and Sexual Diversity in Schreyer, *Web Team Coordinator*, 2020-Present
- Maker Ambassadors, *BUILD Team Member*, 2021-Present